Decomposition of Methane over a Ni−Cu−MgO Catalyst to Produce Hydrogen and Carbon Nanofibers

Haiyou Wang and R. Terry K. Baker*

Catalytic Materials LLC, 1750 Washington St., Holliston, Massachusetts 01746

Received: July 22, 2004; In Final Form: October 13, 2004

We have found that a Ni−Cu−MgO catalyst maintained its activity for the decomposition of methane at high levels for substantially long periods of time at 665−725 °C, being capable of generating large amounts of CO-free H_2 and solid carbon. TEM examinations revealed that the solid carbon consisted exclusively of nanofibers possessing a "platelet" structure, in which the graphite layers are aligned in a direction perpendicular to the axis of the fiber. In sharp contrast, the Ni−MgO−methane system exhibited negligible activity at temperatures ≥650 °C. XRD and H_2 chemisorption characterizations indicated that after reduction a Ni−Cu alloy was formed in the Ni−Cu−MgO catalyst and the surface of the particles was enriched in Cu^0. A possible explanation for the observed superiority of the Ni−Cu−MgO catalyst over that of the Ni−MgO system is presented.

Introduction

Recently, the direct catalyzed decomposition of methane has received great attention as a potential process for the production of CO_x ($x = 1$ or 2)-free hydrogen.[1−14] High-purity hydrogen is extremely desirable for use in proton exchange membrane fuel cells (PEMFC). In addition, methane decomposition (reaction 1)

$$CH_4(g) \rightarrow C(s) + 2H_2(g) \quad \Delta H_{298K} = 74.52 \text{ kJ/mol} \quad (1)$$

is mildly endothermic and emits no CO_2 to the atmosphere. Hence, it is more energy efficient and more environmentally benign than the currently used industrial process, namely, the steam re-forming of methane, followed by CO shift reaction, CO_2 scrubbing, and CO methanation. Furthermore, the direct decomposition of methane also results in the generation of a very important byproduct, carbon nanofibers, a material that has an array of potential applications as electronic components, as polymer additives, and as catalysts/catalyst supports.[15]

To achieve a high concentration of hydrogen in the effluent stream, it is necessary to carry out the reaction at an elevated temperature due to the endothermic nature of methane decomposition. Unfortunately, rapid deactivation of Ni-based catalysts ensues at temperatures in excess of 650 °C, leading to a low yield of hydrogen. It is, therefore, a major challenge to develop a catalyst system that sustains its activity at high temperatures. In the present paper, we report highly promising results on methane decomposition to hydrogen and solid carbon via the use of a Ni−Cu−MgO catalyst, which maintains its activity at high temperatures (665−725 °C) and operates under high space velocity conditions (72 000 mL/h/g of catalyst in terms of the amount of methane flowing through the reactor).

The Cu−Ni system has been the most frequently studied bimetallic catalyst for a variety of reactions and has been the subject of a number of reviews.[16−18] While it is well-established that Cu is capable of enhancing the catalytic activity of Ni, the precise mechanism whereby this phenomenon occurs is still open to considerable debate. Two major rationales have been considered: (a) the modification in the electronic structure that results in surface properties of the bimetallic being different than those of the pure metal and (b) the geometric effect in which ensembles of more than one atom of a given component are less frequently encountered in the surface of a bimetallic than in the pure metal.

A number of studies have focused on the interaction of methane with Cu−Ni catalysts.[19−21] Bernardo and co-workers[19] examined methane decomposition and steam re-forming over silica supported Cu−Ni catalysts over the range 400−600 °C. They reported that in the absence of steam, carbon formation became a major reaction and the deposit took the form of nanofibers. It was found that the morphology of the nanofibers changed from "whiskerlike" (a single fiber associated with a given metal particle) to "octopus" (many fibers from a single particle) as the Cu content of the catalyst was increased from 10 to 80 atom %. In contrast, Kim and co-workers[21] claimed that methane showed no tendency to decompose when passed over unsupported Cu−Ni powders at temperatures below 900 °C. It would appear, therefore, that the presence and nature of the support plays a key role in the Cu−Ni-catalyzed decomposition of methane.

Experimental Section

Materials. The powdered Ni−Cu substrate catalysts were prepared from a thick paste formed by vaporizing most of the solvents included in a slurry consisting of substrate powders and ethanol solutions of nickel and copper nitrates, which was dried overnight at 110 °C and then calcined in an air flow (100 mL/min) for 4 h at 500 °C. The oxide mixture was ground to a fine powder prior to use. The gases used in this work, methane (99.99%), argon (99.999%), and hydrogen (99.99%), were obtained from Air Products Inc. Both the hydrogen and the carrier gas, argon, were purified with Hydro-Purge II and Oxy-Trap columns prior to use. Reagent grade cupric nitrate [$Cu(NO_3)_2 \cdot 2.5H_2O$], nickel nitrate [$Ni(NO_3)_2 \cdot 6H_2O$], MgO (surface

* Corresponding author. Phone: 508-893-9560. Fax: 508-893-9562. E-mail: baker@catalyticmaterials.com.

10.1021/jp040496x CCC: $27.50
Published on Web 11/26/2004

area 106 m^2/g), and SiO_2 (surface area 200 m^2/g) were purchased from Fisher Scientific for the catalyst preparations.

Apparatus and Procedures. The catalytic reactions were carried out in a quartz reactor (i.d. 40 mm) heated by a Lindberg horizontal tube furnace. In a typical experiment, 50.0 mg of powdered catalyst sample was spread along the base of a ceramic boat, which was afterward placed at the center of reactor tube in the furnace. The system was flushed with argon (180 mL/min) for 0.5 h and the catalyst was then reduced in 10% H_2/Ar (200 mL/min) at a temperature between 500 and 1000 °C for 1 h. After reduction, the catalyst was once again flushed with argon (180 mL/min) for 0.5 h. Following this pretreatment, pure methane (60 mL/min, which for 50.0 mg of catalyst corresponds to a space velocity of 72 000 mL/h/g of catalyst) was introduced into the reactor and allowed to interact with the catalyst at a set temperature under atmospheric pressure conditions. The residual feedstock together with gaseous products was analyzed with on-line gas chromatography to determine methane conversion and hydrogen concentration in the effluent. The C and H mass balances were within 5%. The total amount of solid carbon deposited during the reaction was determined gravimetrically after the system had been cooled to room temperature.

The characteristics of the solid carbon products were determined from a combination of transmission electron microscopy (TEM), X-ray diffraction (XRD), and surface area determinations. TEM examinations of the materials were performed in a JEOL 2000EXII instrument (point-to-point resolution of 0.18 nm). Transmission specimens were prepared by ultrasonic dispersion of a small quantity of a given sample in isobutanol and then application of a drop of the suspension onto a holey carbon film. Size distribution profiles were constructed from measurements of over 300 particles in each system. A Rigaku Multiflex X-ray diffractometer with monochromatized Cu Kα radiation was used for the X-ray determinations. The calcined and reduced catalysts were examined at a scanning rate of 1°/min within the 2θ values from 34° to 84°. BET surface areas, calculated from nitrogen adsorption at −196 °C, were carried out on various materials using a Micromeritics TriStar unit. Hydrogen chemisorption experiments were carried out at room temperature in a pulse reactor. During measurement, H_2 was pulsed over the prereduced catalyst until no further adsorption of H_2 was detected. The remaining chemisorbed H_2 was determined quantitatively with a thermal conductivity detector (TCD).

Results

The optimal Ni−Cu−MgO catalyst was found to have a bulk Ni:Cu:Mg molar ratio of 2.4:0.6:1. Figure 1 shows the yields of hydrogen and solid carbon as a function of Cu:Ni molar ratio during methane decomposition over the reduced ($T_{reduction}$ = 850 °C) $Ni_xCu_yMg_zO$ (x:z = 2.4:1) catalysts at 665 °C. In the absence of Cu, the Ni−MgO catalyst exhibited negligible activity under these conditions. On the other hand, the yields of both products increased dramatically as the Cu:Ni ratio was progressively increased from 1/19 to 1/9 and at a more moderate level from 1/9 to1/4. At higher Cu levels the catalytic activity of the system exhibited a sharp decline.

The effect of reduction temperature on the activity and lifetime of the catalyst as well as the yields of hydrogen and solid carbon over the optimal catalyst composition at various reaction temperatures is presented in Table 1. For reaction temperatures ≤700 °C, both the lifetime and the yields increased as the reduction temperature was raised from 600 to 1000 °C,

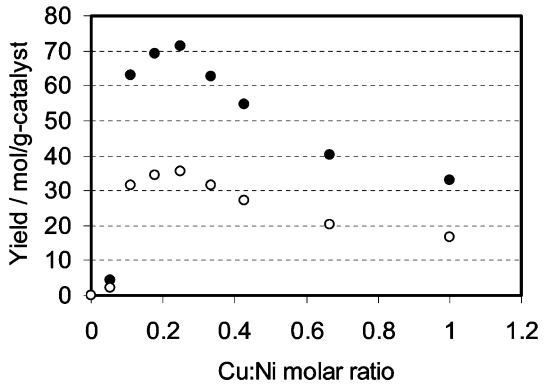

Figure 1. Hydrogen (●) and carbon (○) yields as a function of Cu:Ni molar ratio during methane decomposition over the $Ni_xCu_yMg_zO$ (x:z = 2.4:1) catalysts at 665 °C ($T_{reduction}$ = 850 °C).

TABLE 1: Effect of Reduction Temperature on the Production of Hydrogen and Solid Carbon during Methane Decomposition over the $Ni_xCu_yMg_zO$ (x:y:z = 2.4:0.6:1) Catalyst at Different Temperatures

$T_{reduction}$ (°C)	$T_{reaction}$ (°C)	CH_4 conv[a] (%)	lifetime[b] (h)	yield[c] (mol/g catal)	
				H_2	carbon
600	665	30.7	33	50.2	25.1
700	665	30.5	34	54.5	27.2
850	665	30.6	43	71.2	35.6
1000	665	30.3	45	76.0	38.0
600	700	39.7	24	51.7	25.8
750	700	39.5	26	54.5	27.2
850	700	39.6	29	60.8	30.4
1000	700	39.0	33	70.0	35.0
500	725	46.4	19	42.0	21.0
600	725	46.5	19	43.8	21.9
700	725	45.5	18	42.2	21.1
850	725	44.5	18	38.7	19.3
1000	725	1.1	<1	∼0	∼0
600	750	52.8	11	27.8	13.9

[a] Data obtained after 1 h. [b] Reaction was terminated when the methane conversion was below 5%. [c] Yields were calculated on the basis of the weight of catalyst before reduction.

while the initial methane conversion (after 1 h on stream) remained almost constant. At higher reaction temperatures, ≥725 °C, a catalyst reduction temperature of 600 °C is required in order to achieve the highest product yields. Reduction at temperatures in excess of 600 °C appears to cause a high deactivation rate (a shorter lifetime). By plotting the initial methane conversion vs reaction temperature for a constant reduction temperature (600 or 850 °C), it was found that the initial conversion exhibited a linear relationship with increasing reaction temperature. The highest yields of hydrogen (mol of H_2/g of catalyst) and solid carbon (mol of carbon/g of catalyst) obtained at 665, 700, 725, and 750 °C were 76.0 and 38.0, 70.0 and 35.0, 43.8 and 21.9, and 27.8 and 13.9, respectively. Parts a and b of Figure 2 show the methane conversion and hydrogen concentration in the effluent stream, respectively, as a function of time on stream at different temperatures. It can be seen that, with exception of reactions performed at 750 °C, both methane conversion and hydrogen production remained at high levels for substantially long periods of time. Methane conversion and H_2 concentration were maintained above 30% and 46%, respectively, for 31 h at 665 °C; above 38% and 55%, respectively, for 22 h at 700 °C; and above 44% and 61%, respectively, for 11 h at 725 °C. As a consequence, in addition to H_2, large amounts of solid carbon (its size is significantly

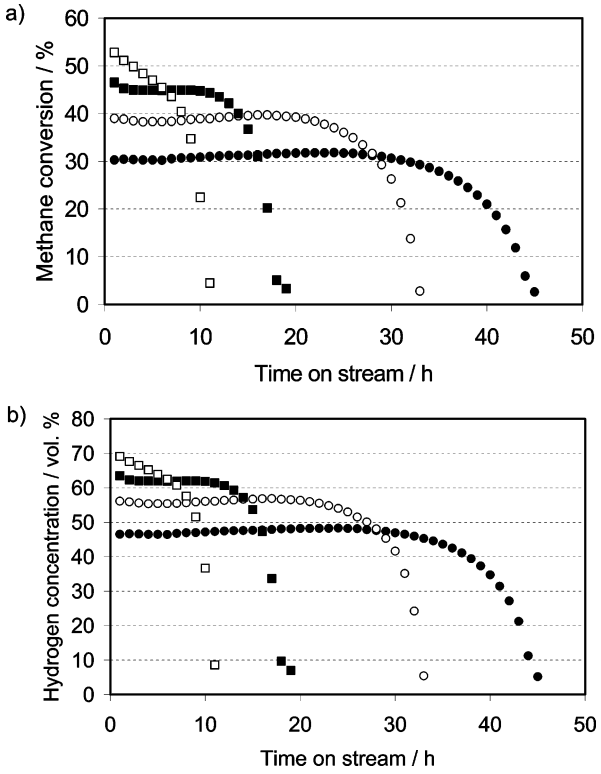

Figure 2. Methane conversion (a) and hydrogen concentration in effluent stream (b) as a function of time on stream during methane decomposition over the $Ni_xCu_yMg_zO$ (x:y:z = 2.4:0.6:1) catalyst at 665 °C (□), 700 °C (■), 725 °C (○), and 750 °C (●) ($T_{reduction}$ = 1000 °C for 665 and 700 °C; $T_{reduction}$ = 600 °C for 725 and 750 °C).

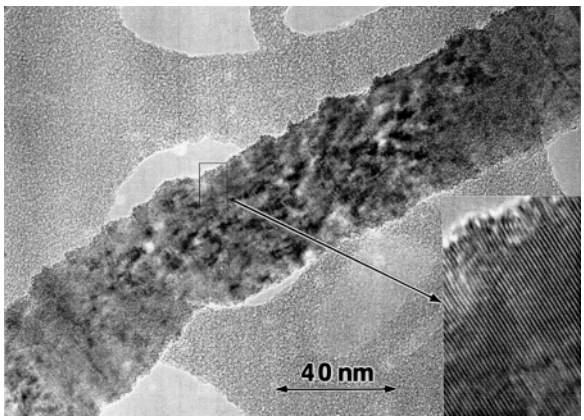

Figure 3. High-resolution TEM photograph of a carbon nanofiber formed during methane decomposition over the $Ni_xCu_yMg_zO$ (x:y:z = 2.4:0.6:1) catalyst at 665 °C ($T_{reduction}$ = 1000 °C).

greater than that of the charged catalyst) were generated during the steady-state period at temperatures between 665 and 725 °C.

TEM examinations revealed that the solid carbon product consisted exclusively of nanofibers when methane decomposition was carried out over the Ni−Cu−MgO catalyst. From measurements of over 300 nanofibers it was possible to determine that these materials had an average width of 40 nm and typical lengths of 5−10 μm. Inspection of the high-resolution TEM micrograph (Figure 3) shows that the nanofibers possess a "platelet" structure, in which the graphite layers are aligned in a direction perpendicular to the growth axis of the fiber.[22]

In an attempt to gain an insight into the observed superiority of the Ni−Cu−MgO catalyst over that of the Ni−MgO system, H_2 chemisorption and XRD experiments were carried out. After a reduction at 850 °C, the amounts of H_2 chemisorbed on the $Ni_xCu_yMg_zO$ (x:y:z = 2.4:0.6:1) and the Ni_xMg_zO (x:z = 2.4:1) systems were 12.8 and 291.5 μL (STP)/g of catalyst, respectively. XRD patterns of the calcined and reduced $Ni_xCu_yMg_zO$ (x:y:z = 2.4:0.6:1) catalyst samples are presented in Figure 4. The XRD peaks of the calcined catalyst can be assigned to MgO and any of the following compounds: NiO, (Ni, Cu)O, (Ni, Mg)O, and (Ni, Cu, Mg)O (Figure 4a). For the reduced sample, a Ni−Cu alloy rather than independent Ni and Cu species was identified and the intensities of the peaks from the Ni−Cu alloy were seen to strengthen with increasing reduction temperature (Figure 4b−d). The estimated crystallite size of the Ni−Cu alloy in the $Ni_xCu_yMg_zO$ (x:y:z = 2.4:0.6:1) catalyst, based on the width of the XRD peak of the (200) face, was found to increase from about 17 to 35 nm as the reduction temperature was progressively raised from 600 to 1000 °C (30 nm at 850 °C). The estimated crystallite size of Ni in the Ni_xMg_zO (x:z = 2.4:1) catalyst sample after reduction at 850 °C was found to be about 28 nm. It is significant to find that after a reduction at 850 °C the crystallite sizes of metal particles in both catalysts are very close, whereas the amount of H_2 adsorbed over the Ni_xMg_zO (x:z = 2.4:1) catalyst is about 23 times greater than that over the $Ni_xCu_yMg_zO$ (x:y:z = 2.4:0.6:1) sample. This finding suggests that the surface of the latter catalyst is enriched in Cu^0, a claim that is consistent with previous work.[18]

Discussion

During the catalytic hydrocarbon decomposition reaction, methane molecules are initially adsorbed and decomposed on the metal surface of the catalyst particle, resulting in the formation of chemisorbed carbon species and the release of gaseous hydrogen; the carbon species proceed to dissolve and diffuse through the bulk of the metal particle, ultimately leading to precipitation of carbon at the rear of the metal particle and the formation of a nanofiber with an exposed metal particle remaining at its tip. Deactivation occurs when the rate of carbon diffusion through the metal catalyst particles is slower than that of the formation of carbon at the surface Ni^0 sites.[23] Under these circumstances, carbon builds up at the catalyst surface and eventually encapsulates the particle and the growth of nanofibers ceases.

When the Ni−Cu−MgO catalyst is exposed to a methane atmosphere, the initial carbon formation rate is not expected to be rapid, since at this stage there are relatively few exposed Ni^0 sites present at the particle surfaces. As a consequence, the catalyst can survive during the early stages of the reaction. As the reaction proceeds, there is an enhancement in the number of surface Ni^0 sites due to the selective and strong interaction that exists between methane and nickel (copper is inactive for methane adsorption and decomposition), and a balance is established between the generation of carbon at these regions and its bulk diffusion through the particle. As a consequence, the catalyst is able to maintain its high activity for a substantially long period of time at a high reaction temperature, and substantial yields of hydrogen and solid carbon can be realized (Figures 1 and 2). In sharp contrast, the Ni−MgO catalyst system undergoes rapid deactivation upon interaction of the particles with methane due to the presence of a large number of exposed Ni^0 sites, resulting in negligible yields of hydrogen and solid carbon (Figure 1).

It is significant to find that if methane is passed over silica-supported Cu−Ni or Ni particles at temperatures of about 500 °C, then both systems generate carbon nanofibers.[19,24] To understand the difference in behavior of Cu−Ni and Ni when

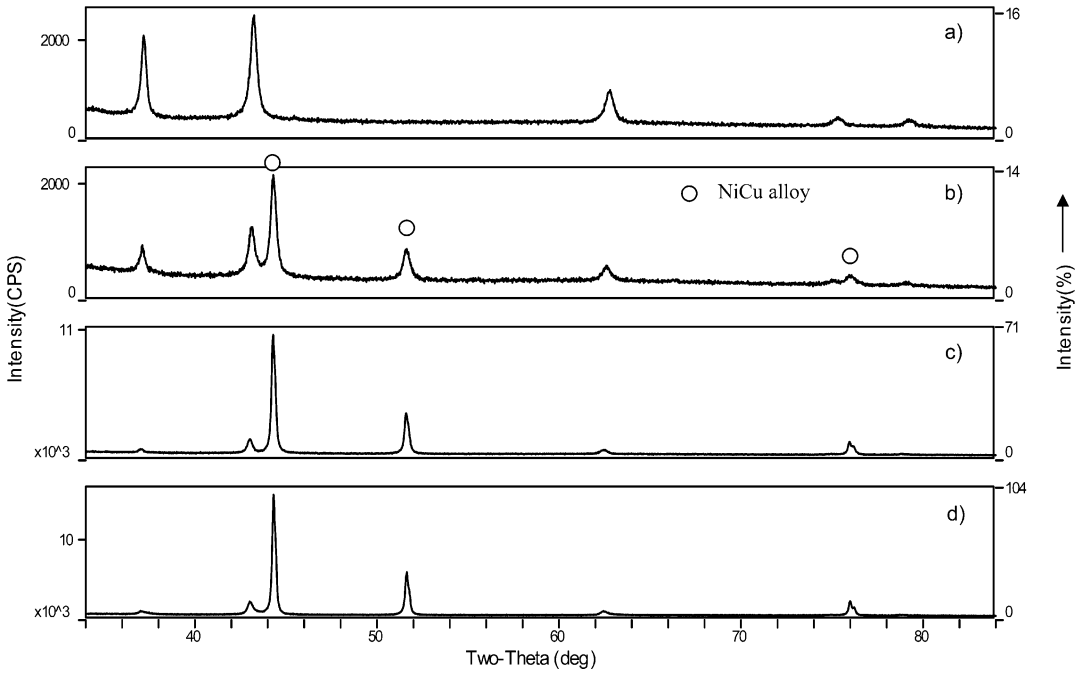

Figure 4. XRD patterns of the $Ni_xCu_yMg_zO$ (x:y:z = 2.4:0.6:1) catalysts after calcination at 500 °C (a), after reduction at 600 °C (b), after reduction at 850 °C (c), and after reduction at 1000 °C (d).

TABLE 2: Effect of Substrate on the Production of Hydrogen and Solid Carbon during Methane Decomposition over the Ni−Cu (4:1)-Based Catalysts Reduced at 600 °C and Reacted at 725 °C

substrate	CH_4 conv[a] (%)	lifetime[b] (h)	yield[c] (mol/g catal) H_2	yield[c] (mol/g catal) carbon
none	0	0	0	0
SiO_2	38.5	9	17.2	8.6
MgO	46.5	19	43.8	21.9

[a] Data obtained after 1 h. [b] Reaction was terminated when methane conversion was below 5%. [c] Yields were calculated on the basis of the weight of catalyst before reduction.

supported on SiO_2 or MgO with regard to the reaction with methane, it is necessary to examine the nature of respective metal−support interactions.

The choice of the MgO component in the catalyst was another critical aspect. As seen from the data presented in Table 2, at a reaction temperature of 725 °C, in the absence of MgO, the Ni_xCu_y (x:y = 4:1) catalyst provided no activity for methane conversion, indicating the necessity of the presence of MgO as both a chemical component and dispersing agent in the catalyst. Furthermore, as seen in Table 2, the substitution of MgO by SiO_2 resulted in formation of a catalyst that exhibited a lower initial methane conversion level and a shorter lifetime with the concomitant generation of lower amounts of hydrogen and solid carbon. The superior performance obtained with a catalyst containing MgO is most likely related to the tendency to form less reducible (Ni, Mg)O and (Ni, Cu, Mg)O solid solutions in the Ni−Cu−MgO system during the calcination step, which subsequently creates metallic particles of smaller size over MgO following reduction. We have observed that at a reaction temperature of 725 °C the Ni−Cu−MgO catalyst reduced at a temperature higher than 600 °C exhibited shorter lifetimes (Table 1) and the crystallite size of the Ni−Cu alloy was found to increase with increasing reduction temperature. Indeed, estimates based on the width of the XRD peak of the (200) face indicate that the crystallite sizes of the Ni−Cu alloys in the Ni−Cu−SiO_2 and Ni−Cu−MgO catalysts were 35 and 17 nm, respectively, after a reduction at 600 °C.

The metal crystallite size is a further factor that exerts an impact on the catalyst stability. It is generally agreed that diffusion of carbon through the catalyst particle is the rate-determining step in the growth of carbon nanofibers.[23] At a given temperature, the rate of nanofiber elongation is inversely proportional to the square of the particle size.[25] On the other hand, for a given sized metal particle, the rate of carbon diffusion increases exponentially with increasing reaction temperature. Consequently, the diffusion of carbon through the metal particle is affected not only by the reaction temperature but also by the size of metal particles and so is the stability (lifetime) of the catalyst. It is of interest to contrast this behavior with that found for the growth of carbon nanotubes, where the surface diffusion of carbon around the catalyst particle is purported to be the rate-controlling step.[26] In this context, it should be appreciated that the latter structures are believed to be hollow, whereas the "platelet" graphite nanofibers are completely solid materials. Indeed, as shown in Table 1, for a constant reduction temper-

TABLE 3: Comparison of the Physical and Structural Characteristics of "Platelet" Carbon Nanofibers Produced from Different Catalytic Reactions[a]

catalyst	feedstock	space velocity (mL/h/g of catalyst)	GNF yield (g of C/g of catalyst)	average width (nm)	d-spacing (nm)	surface area (m^2/g)
$Ni_xCu_yMg_zO$ (x:y:z = 2.4:0.8:1)	CH_4	72 000	381	38.0	0.3389	216
Cu-Fe (3:7)	CO/H_2 (4:1)	240 000	42	110.0	0.3359	76

[a] $T_{reaction}$ = 665 °C.

ature the lifetime of the Ni−Cu−MgO catalyst was strongly dependent upon the reaction temperature. In addition, XRD measurements indicated that the crystallite size of Ni−Cu alloy particles in the Ni−Cu−MgO catalyst increased as a function of reduction temperature. This aspect accounts for the finding that for a constant reaction temperature the stability of the catalyst was also strongly influenced by the reduction temperature (Table 1). Furthermore, the fraction of surface Ni^0 sites in the Ni−Cu−MgO catalyst is enhanced during reaction and the final composition of the particle surface is dependent upon the reaction temperature. Therefore, methane conversion is not only affected by the reaction temperature but also by the ultimate number of surface Ni^0 sites that the hydrocarbon encounters during adsorption on the particle surface. This rationale accounts for why the initial methane conversion did not exhibit an exponential increase with reaction temperature for a constant reduction temperature (Table 1).

A further fascinating aspect that emerges from this investigation concerns the structural characteristics of the carbon nanofibers generated from the Ni−Cu−MgO/CH_4 reaction. The finding that the nanofibers adopt a "platelet" conformation is totally unexpected, since the interaction of this particular bimetallic composition with other hydrocarbons always leads to the formation of "herringbone" structures.[21,27] Indeed, the formation of "platelet" nanofiber structures has generally been reported from reactions where CO has been passed over an iron-containing catalyst.[23−30] It would appear that the chemistry involved in the interaction of the Ni−Cu−MgO system creates metal particles that adopt specific crystallographic orientations that favor the precipitation of carbon in the form of graphite sheets that are aligned in a direction perpendicular to the longitudinal axis of the fiber.

A comparison is given in Table 3 of the respective yields and physical and structural characteristics of "platelet" graphite nanofibers grown from the decomposition of CH_4 over $Ni_xCu_yMg_zO$ (x:y:z = 2.4:0.8:1) at 665 °C with similar materials synthesized from the interaction of Cu−Fe (3:7) with CO/H_2 at the same temperature.[30] Inspection of these data reveals that by using the new catalyst system one can synthesize "platelet" graphite nanofibers having a significantly narrower width than those grown from the traditional catalyst. It is also evident that the van der Waals forces are weaker as the width of the structures decreases, and as a consequence, the spacing between adjacent graphite layers increases. The smaller dimensions of the nanofibers generated from the new catalyst system is also reflected in a larger value of the surface area.

References and Notes

(1) Pourier, M. G.; Sapundzhiev, C. *Int. J. Hydrogen Energy* **1997**, *22*, 429.
(2) Zhang, T.; Amiridis, M. D. *Appl. Catal. A: Gen.* **1998**, *167*, 161.
(3) Muradov, N. Z. *Energy Fuels* **1998**, *12*, 41.
(4) Aiello, R.; Fiscus, J. E.; zur Loye, H.-C.; Amiridis, M. D. *Appl. Catal. A: Gen.* **2000**, *192*, 227.
(5) Ermakova, M. A.; Ermakov, D. Yu.; Kuvshinov, G. G. *Appl. Catal. A: Gen.* **2000**, *201*, 61.
(6) Li, Y.; Chen, J.; Qin, Y.; Chang, L. *Energy Fuels* **2000**, *14*, 1188.
(7) Muradov, N. *Int. J. Hydrogen Energy* **2001**, *26*, 1165.
(8) Choudhary, T. V.; Sivadinarayana, C.; Chusuei, C. C.; Klinghoffer, A.; Goodman, D. W. *J. Catal*. **2001**, *199*, 9.
(9) Takenaka, S.; Ogihara, H.; Yamanaka, I.; Otsuka, K. *Appl. Catal. A: Gen.* **2001**, *217*, 101.
(10) Shah, N.; Panjala, D.; Huffman, G. P. *Energy Fuels* **2001**, *15*, 1528.
(11) Piao, L.; Li, Y.; Chen, J.; Chang, L. J.; Lin, Y. S. *Catal. Today* **2002**, *74*, 145.
(12) Ermakova, M. A.; Ermakov, D. Yu. *Catal. Today* **2002**, *77*, 225.
(13) Takenaka, S.; Shigeta, Y.; Otsuka, K. *Chem. Lett*. **2003**, *32*, 26.
(14) Villacampa, J. I.; Royo, C.; Romeo, E.; Montoya, J. A.; Del Angel, P.; MonzÓn, A. *Appl. Catal. A: Gen.* **2003**, *252*, 363.
(15) De Jong, K. P.; Geus, J. W. *Catal. Rev.-Sci. Eng.* **2000**, *42*, 481.
(16) Khulbe, K. C.; Mann, R. S. *Catal. Rev.-Sci. Eng*. **1982**, *24*, 311.
(17) Ponec, V. *Int. Quantum Chem.* **1977**, *12*, 1.
(18) Sinfelt, J. H. *Acc. Chem. Res*. **1977**, *10*, 15.
(19) Bernardo, C. A.; Altrup. I.; Rostrup-Nielsen, J. R. *J. Catal*. **1985**, *96*, 517.
(20) Tavares, M. T.; Bernardo, C. A.; Altrup, I.; Rostrup-Nielsen, J. R. *J. Catal*. **1986**, *100*, 545.
(21) Kim, M. S.; Rodriguez, N. M.; Baker, R. T. K. *J. Catal*. **1991**, *131*, 60.
(22) Rodriguez, N. M.; Chambers, A.; Baker, R. T. K. *Langmuir* **1995**, *11*, 3862.
(23) Baker, R. T. K.; Barber, M. A.; Harris, P. S.; Feates, F. S.; Waite, R. J. *J. Catal*. **1972**, *26*, 51.
(24) Rostrup-Nielsen, J. R. *J. Catal*. **1972**, *10*, 221.
(25) Baker, R. T. K. In *Gas Chemistry in Nuclear Reactors and Large Industrial Plant*; Dyer, A., Ed.; Heyden: 1980; p 18.
(26) Helveg, S.; Lopez-Cartes, C.; Sehested, J.; Hansen, P. L.; Clausen, B. S.; Rostrup-Nielsen, J. R.; Abild-Pedersen, F.; Norskov, J. K. *Nature* **2004**, *427*, 426.
(27) Marotta, C. L.; Baker, R. T. K. *J. Mol. Catal. A: Chem.* **2003**, *195*, 209.
(28) Murayama, H.; Maeda, T. *Nature* **1990**, *345*, 791.
(29) Rodriguez, N. M.; Kim, M. S.; Baker, R. T. K. *J. Catal*. **1993**, *144*, 93.
(30) Carneiro, O. C.; Kim, M. S.; Yim, J. B.; Rodriguez, N. M.; Baker, R. T. K. *J. Phys. Chem. B* **2003**, *107*, 4237.